Nonmetal-metal transition in metal–molten-salt solutions

Pier Luigi Silvestrelli*
Stichting voor Fundamenteel Onderzoek der Materie, Institute for Atomic and Molecular Physics, Kruislaan 407, 1098 SJ Amsterdam, The Netherlands

Ali Alavi
Atomistic Simulation Group, School of Mathematics and Physics, The Queen's University, Belfast BT7 1NN, Northern Ireland, United Kingdom

Michele Parrinello
Max-Planck-Institut für Festkörperforschung, Heisenbergstrasse 1, 70569 Stuttgart, Germany

Daan Frenkel
Stichting voor Fundamenteel Onderzoek der Materie, Institute for Atomic and Molecular Physics, Kruislaan 407, 1098 SJ Amsterdam, The Netherlands

(Received 20 November 1995; revised manuscript received 17 January 1996)

The method of *ab initio* molecular dynamics, based on finite-temperature density-functional theory, is used to study the nonmetal-metal transition in two different metal–molten-salt solutions, $K_x(KCl)_{1-x}$ and $Na_x(NaBr)_{1-x}$. As the excess metal concentration is increased the electronic density becomes delocalized and percolating conducting paths are formed, making a significant dc electrical conductivity possible. This marks the onset of the metallic regime. By calculating several electronic and structural properties, remarkable differences between the two solutions are observed. The anomalous behavior of $Na_x(NaBr)_{1-x}$, typical of all the Na-Na*X* solutions, is found to be related to the strong attractive interaction between the sodium ions and the excess electrons. [S0163-1829(96)01519-6]

I. INTRODUCTION

The nonmetal-metal (NM-M) transition occurs in many condensed matter systems such as metal–molten-salt solutions, metal-ammonia solutions, doped semiconductors, expanded liquid metals, and metal clusters.[1] The transition can be induced by changes in thermodynamic parameters such as temperature, pressure, concentration, and composition.

While a considerable amount of work has already been devoted[1] to the NM-M transition in disordered systems, our understanding of the transition at the microscopic level is still far from complete. In particular, the detail of the interaction between electronic and structural properties, the possibility of electron localization within well-identified chemical structures or by disorder effects, and the exact role of the concentration fluctuations related to the liquid-liquid phase separation, often observed in the vicinity of the electronic transition, remain an area open to investigation.

Among the systems where the NM-M transition has been observed, metal–molten-salt solutions of the type $M_x(MX)_{1-x}$ have been studied extensively through experiments,[2–11] computer simulations,[12–15] and theory.[1,16–18] The alkali metals dissolve in molten alkali halides to form true solutions. In most cases the phase diagrams of these systems show a critical point above which the two liquids are completely miscible.[2] The electrical conductivity of the solution changes with concentration from that of an ionic liquid to that of a liquid metal. A problem of great interest in such NM-M transition is the manner in which the change from localized to extended electronic states occurs.[16–18] The established picture is that at very low x the valence electrons of the added metal are released in the salt and are localized into liquid cavities (F centers). As the concentration is increased spin-paired states (bipolarons) and higher aggregates are formed, the onset of metallic behavior being related to the formation of percolating bipolaronic clusters.

The approach to metallic regime in $K_x(KCl)_{1-x}$ has been studied numerically by Fois, Selloni, and Parrinello[15] Their simulations were carried out using *ab initio* molecular dynamics (MD). In such simulations, density-functional theory (DFT) in the local-density approximation (LDA) is used to compute the ground-state electronic properties of the system. Moreover, the method of Ref. 15 is based on the Born-Oppenheimer (BO) approximation, namely, it is assumed that the electrons adiabatically follow the nuclear motion. However, due to the low concentration of carriers and to the relatively high temperature, the Fermi energy E_F is of the same order of the thermal energy k_BT and, by increasing the metal concentration, the electronic excitation energy becomes also comparable to k_BT. This leads to fractional occupation numbers and to a finite probability of occupation of the excited states so that the hypothesis of BO behavior is questionable and therefore the possibility exists that computed quantities give a poor description of the physics of the system. Indeed, by performing a simulation at $x=0.11$, Fois Selloni, and Parrinello[15] obtained a dc electrical conductivity considerably larger than the experimental value. Furthermore, they had severe difficulties in maintaining the system on the BO energy surface and this prevented them from

studying the solution at $x>0.11$ that is in the concentration region where the system exhibits a true metallic behavior.

Recently an alternative formulation of the density-functional-based MD, which is able to circumvent these problems, has been proposed by Alavi *et al.*[19] It is based on a density functional which shares the same *stationary* point as the finite-temperature functional of Mermin,[20] and incorporates consistently the effects of thermal electronic excitations and fractionally occupied states.

We have applied this method to study the change of the electronic and structural properties of $K_x(KCl)_{1-x}$ in the approach to the metallic regime induced by the increase of the excess metal concentration x. In particular, we have studied the behavior of the electronic states near the Fermi energy. These states are localized in the insulator and become spatially extended in the metal giving rise to percolating structures and making electronic conduction possible. Moreover we have studied $Na_x(NaBr)_{1-x}$ at different excess metal concentrations by comparing its properties with those of $K_x(KCl)_{1-x}$. Na solutions show a characteristic anomalous behavior since some properties differ significantly from those of the heavier alkali metals.[2,5,11,21–24] In particular, the electronic conductivity has a sublinear dependence on x over a range of temperatures, a feature which is not observed in the other solutions.[2]

The outline of the paper is as follows. In Sec. II we briefly review the NM-M transition in metal–molten-salt solutions. In Sec. III we describe the Na-NaX solution anomalous behavior. Section IV presents our algorithm and provides computational details. Section V is devoted to results and discussion. Finally, our conclusions are presented in Sec. VI.

II. THE NM-M TRANSITION IN METAL–MOLTEN-SALT SOLUTIONS

A great deal of experimental work has been devoted to study the NM-M transition in metal–molten-salt solutions.[2–11] Low concentrations of excess electrons are localized.[25] In principle different configurations are possible: neutral alkali atoms, multisite localized states, and F centers. Optical-absorption[6] and NMR (Ref. 25) studies of dilute concentrations of excess electrons provide considerable support for the F-center model. The F-center model has been also confirmed by MD calculations.[12] It was found that an electron released in molten KCl rapidly localizes and is coordinated by roughly four cations. Although at low concentration, the electrons are localized, some of them at least are sufficiently mobile to provide the observed electronic conductivity.[2,9,25] Because the optical transition energies and, hence, the binding energies in the static liquid structure greatly exceed thermal energies, such rapid transport of F-center electrons inevitably requires substantial help from ionic motions. Such a mechanism, which allows the electrons to escape from the F-center potential well, may be viewed as analogous to polaron motion in solids, but it is likely to involve diffusive as well as vibrational motions. A transport mechanism of this character has been observed in simulations by Selloni *et al.*[13] Their results show F-center electrons jumping to a new location after a time of the order of 0.3 ps, as a result of ionic motions.

As the concentration is increased spin pairing occurs and a new complex (the bipolaron) is formed: electrons with opposite spins bind and localize in a cavity that closely resembles that of an F center. In other words, they sit in an anion vacancy, and surround themselves on the average by four cations. At low metal concentrations the optical study of Nattland, Rauch, and Freyland[11] is consistent with a dynamical equilibrium between F centers and bipolarons, and the formation of bipolarons in a singlet state is strongly supported by the behavior of measured static magnetic susceptibilities.[4] The bipolaronic complexes[15] are a characteristic motif of the melt, which tends to preserve the molten-salt structure by replacing the missing X^- ions with bipolarons. This tendency may explain the stability of the molten- salt ionic structure to the addition of metal.[26]

At still higher concentrations the bipolarons tend to cluster. In particular, MD simulations[15] show that for $x=0.06$ the clusters are mostly localized, while for $x=0.11$ the dominant structure is a percolating electronic charge distribution, i.e., an elongated distribution extending from one side to the other of the simulation cell. Obviously the appearance of percolating paths has important consequences for the electronic properties of the system. In fact the highest occupied molecular orbital-lowest unoccupied molecular orbital (HOMO-LUMO) energy gap is reduced and the electron states near the Fermi energy become delocalized so that an appreciable increase of the dc electrical conductivity σ occurs. In this way the system undergoes a NM-M transition. As x tends to 1, σ continues to increase towards its liquid metal value.

Different theoretical and experimental approaches lead to very similar values for the percolation threshold in $K_x(KCl)_{1-x}$.[4,8,10,18,27] The observed infrared dielectric anomaly[6] could indicate that the NM-M transition may occur at a metal concentration as low as $x\simeq 0.1$; however, this transition should really appear through a divergence of the static dielectric constant.[28] More probably[18] the anomaly simply indicates the appearance of sizable metallic clusters, the system as a whole still being in a nonmetallic state.[29,30] Nattland, Heyer, and Freyland[8] located the separation point between metallic and nonmetallic transport regime near $x=0.23$, by studying the temperature coefficient of the dc electrical conductivity. According to the Faber-Ziman theory[31] of liquid metals, a negative value of $\partial\ln\sigma/\partial T$ is consistent with nearly-free-electron transport. On the other end, thermally activated transport is signalled by a positive temperature dependence of σ. So above $x\simeq 0.2$ delocalization of the electronic states should be complete. The magnitude of σ at $x=0.2$ reaches a value[8] of about 150 Ω^{-1} cm^{-1}, which is comparable to the Mott minimum metallic conductivity.[16] If electron localization by disorder is one of the basic features of the transition, this minimum metallic conductivity often has been invoked as a possible NM-M transition criterion.[1] Garbade and Freyland[10] found an exceptional S-shape behavior of the molar excess volume. Its changing from positive to negative values, near $x\simeq 0.2$, could indicate the onset of the metallic regime. Senatore and Tosi[18] have considered the volume percolation problem to describe the NM-M transition and, for K_xKCl_{1-x}, they calculated a percolation threshold of $x=0.21$. This estimate agrees with the concentration behavior of the static magnetic susceptibility:[4] in $K_x(KCl)_{1-x}$ the molar susceptibility of dissolved metal

approaches the Pauli-Landau value of the pure bulk metal near $x=0.2$. Finally, Morgan, Gilbert, and Hickey[27] found that localization, indicated by the divergence of the transport relaxation rate, should set in at $x=0.15$.

III. ANOMALOUS BEHAVIOR IN SODIUM

The clear distinction in the concentration dependence of the electronic conductivity between Na-NaX and K-KX systems was pointed out first by Bronstein and Bredig some 40 years ago.[21] The sublinear dependence on x of the electrical conductivity could be related to the formation of long-lived nonmagnetic and nonconducting species.[5] The effect of such species is to remove excess electrons from the conduction process. As possible candidates, the formation of Na_2 molecules[21] and/or Na^- ions has been suggested.[5] Furthermore, in Na-NaBr, the optical absorption spectrum, which is usually considered the strongest evidence in favor of the F-center model, has a number of peculiar features.[23] The peak energy does not satisfy the Mollwo-Ivey relation, as in the other solutions. The spectrum is particularly broad and can be deconvoluted into two separate bands centered at 1.4 and 1.8 eV, whose origin is not clear.

Xu, Selloni, and Parrinello[22] showed, by a quantum molecular dynamics method, that several features of the peculiar behavior of dilute Na-NaBr solutions can be related to the formation of dipolar atomic states that differ from the F-center-like complexes found in dilute solutions of heavier alkali metals. This dipolar atomic picture is similar to that proposed by Logan[32] and offers a simple clue to understanding the optical spectrum. Xu, Selloni, and Parrinello[22] also showed that the greater strength of the sodium ion-electron potential is mostly responsible for the different behavior of the electronic states in Na-NaBr. In particular, they found a substantial difference between the radial electron ion pair correlation functions of Na-NaBr and K-KCl, the electron states being much more localized and atomiclike in Na-NaBr. This is in agreement with experiments[11] which show a clear difference in the nature of localization reflected by the comparison of optical spectra for Na-NaX and K-KX. Xu, Selloni, and Parrinello[22] considered two electrons with antiparallel spins and found that they are most frequently close to a single Na^+ ion, thus forming a Na^- species with a pronounced dipolar character. However, other species are also observed, most noticeably Na_2 molecules and bipolaronlike complexes. All these spin-paired species change into one another via two different mechanisms. The first mechanism is ionic diffusion, which continuously causes the evolution of one species into another, sometimes making the distinction between the different species arbitrary. The second mechanism occurs via jumps which lead to dissociation of the current species and to successive recombination either in the same spatial position or in a different one. Basically, Xu, Selloni, and Parrinello[22] found that the structure of the electron states in dilute metal-metal halide solutions is not uniquely F center like but depends on the strength of the potential of the alkali-metal ions. When this potential is sufficiently strong atomiclike states with some dipolar character appear to be favored with respect to the F center.

IV. COMPUTATIONAL SCHEME

Simulations have been carried out using the method of *ab initio* MD, based on finite-temperature density-functional theory, proposed by Alavi *et al.*[19] The system is modeled as a collection of N_e excess electrons, 108 cations M^+ (K^+ or Na^+), and $(108-N_e)$ anions X^- (Cl^- or Br^-). Only the N_e electrons are treated quantum mechanically, the effect of the remaining ''core'' electrons being taken into account by using suitable ion-ion and electron-ion pseudopotentials. We have performed simulations, with $N_e=$ 2, 6, 12, 16, 18, 24 for K-KCl, and $N_e=$ 2, 10, 18 for Na-NaBr. These values correspond to an excess metal concentration of $x=0.02$, 0.06, 0.11, 0.15, 0.17, 0.22 in K-KCl, and of $x=0.02$, 0.09, 0.17 in Na-NaBr, respectively. In each case the temperature was $T\sim 1300$ K and the molar volume was taken equal to the corresponding experimental value[2,10] at $x=0$, since it is almost independent[10] of the excess metal concentration in the range of values studied. In our system periodic boundary conditions were imposed, the simulation box being a cube of length 39.0 a.u. for K-KCl, and 38.3 a.u. for Na-NaBr. The electronic orbitals, at the Γ point of the Brillouin zone, were expanded in plane waves on a mesh of $(16)^3$. Previous tests[15] established the adequacy of this choice. The pseudopotentials used to describe the ion-ion and electron-ion interactions were the same as in Refs. 12–15, 22. The interaction between the ions is modeled by a pairwise long-range Coulomb interaction term plus a Born-Mayer (exponential) repulsive term,

$$V_{IJ}(r)=\frac{Z_I Z_J e^2}{r}+A_{IJ}e^{-r/\rho_{IJ}}. \tag{1}$$

The long-range part of this potential is treated by the Ewald summation method and the parameters A, ρ are those fixed by Fumi and Tosi.[33] The electron-ion pseudopotentials have the following form:

$$V_{eI}(r)=-\frac{Z_I e^2}{r}\mathrm{erf}(r/C_I). \tag{2}$$

This function is a smoothed version of the Shaw pseudopotential.[34] Such smoothing is required by the use of a discrete mesh to represent the density and does not introduce any significant quantitative effect. This was explicitly checked, in the case of a single solvated electron, by Selloni *et al.*[13] C is a measure of the radius of the ion core: for $r\gg C$ the potential is Coulombic, while for $r\ll C$ the potential is a constant. The radius of the anion is not very critical in the calculation, because the electrons do not get close to the anions; $C=2.2$ a.u. was used both for Cl^- and Br^-. In contrast the radius of the cation is crucial since it determines the binding energy of the electron. It is chosen to approximately fit the atomic ionization potential. In our simulations $C=3.7$ a.u. (Refs. 12 and 14) and $C=3.0$ a.u. (Ref. 22) for K^+ and Na^+, respectively. The pseudopotential of Eq. (2) is certainly not up to the present state of the art in the field but it has the advantage of simplicity and of having been extensively tested in the study of metal–molten-salt solutions. Furthermore it is fully local, which allows us to use the method of Ref. 19, which has so far been formulated only for the case of local potentials.

For a given configuration of ions, the electronic density $n(\mathbf{r})$ was computed by minimizing the free energy functional $\mathscr{F}$ of the electron gas. This is defined as

$$\mathscr{F}=\Omega+\mu N+E_{II}, \tag{3}$$

where

$$\Omega[n(\mathbf{r})]=-\frac{2}{\beta}\ln\det(1+e^{-\beta(\mathscr{H}-\mu)}) - \int d\mathbf{r}n(\mathbf{r})\left(\frac{\phi(\mathbf{r})}{2}+\frac{\delta\Omega_{\rm xc}}{\delta n(\mathbf{r})}\right)+\Omega_{\rm xc}, \tag{4}$$

$\beta=1/k_BT$ is the inverse electronic temperature, μ is the chemical potential, $\mathscr{H}=-\hbar^2/2m\nabla^2+V(\mathbf{r})$ is the one-electron Hamiltonian with the effective potential $V(\mathbf{r})=\Sigma_I V_{eI}(\mathbf{r}-R_I)+\phi(\mathbf{r})+\delta\Omega_{\rm xc}/\delta n(\mathbf{r})$, $\phi(\mathbf{r})$ is the Hartree potential of an electron gas of density $n(\mathbf{r})$, $\Omega_{\rm xc}$ the LDA exchange-correlation energy, which is approximated by its $T=0$ value, and E_{II} the classical Coulomb energy of the ions. For the exchange-correlation part of the electron-electron interaction the expression of Ceperley and Alder is used.[35]

$\mathscr{F}$ reproduces the exact finite-temperature density of the Mermin functional[20] and was optimized for each ionic configuration using a self-consistent diagonalization method, as in Ref. 19. The electronic density so computed, together with the Hellmann-Feynman theorem, enables the calculation of the ionic forces. In this approach the electrons are allowed to be in thermal equilibrium with the ions (hot electrons), while, in contrast, in the BO approximation, the electrons are kept artificially cold. The ionic degrees of freedom were integrated using a time step of 20 a.u. ($\sim$0.5 fs). The first part of each simulation was the preparation of a well-equilibrated liquid of M^+ and X^- ions in a neutralizing uniform background ($\sim$2 ps); then the uniform background was removed and, for each ionic configuration, $\mathscr{F}$ was self-consistently optimized by using as the electronic temperature the average ionic temperature, namely, 1300 K. After an equilibration of 0.5 ps a production run of 2 ps was performed.

V. RESULTS AND DISCUSSION

A. Pair correlation functions

To characterize the structure of the ionic liquid we computed the ion-ion radial pair correlation functions of K-KCl, at five different excess metal concentrations. These functions do not change very much, by increasing the x value. In particular, the cation-anion correlation function, $g_{+-}(r)$ (see Fig. 1), is only slightly affected by variations of x. The ion-ion radial pair correlation functions of Na-NaBr exhibit an analogous trend. This is in agreement with the experiments[26] which indicate that the molten-salt structure persists up to very high excess metal concentrations. Accordingly, the mean coordination number Z_{+-}, calculated by integration of $g_{+-}(r)$ up to the first minimum, remains close to six for each x.

In Table I we report the averaged cation–closest-cation distance, R_{++}, as a function of x, for K-KCl. This quantity, computed by integration of the cation-cation correlation function, $g_{++}(r)$, shows a characteristic behavior. By increasing x, it decreases, reaches a minimum value around $x=0.15$, and then it starts increasing. This behavior could be explained as follows. For low x the molten-salt structure is almost perfect. By increasing x, the electron charge tends to bring the metal-alkali ions closer to each other. This effect is maximum at a certain metal concentration. For still higher x values R_{++} becomes larger since the system is approaching the liquid-metal regime, which should be characterized by a fairly homogeneous ionic distribution. The onset of delocalized electronic states, that is, the NM-M transition point, could be connected with the beginning of the increase of R_{++}, at $x\simeq0.15$. An effect which may be related has been reported by Garbade and Freyland,[10] who measured the phase diagram of K-KCl over the whole composition range. They have studied the behavior of the excess metal partial molar volume $\overline{V}_{\rm K}(x)$. Its initial reduction, at low metal concentrations, is consistent[10] with localized electronic states in the form of F centers and F-center aggregates like dimers. On the other hand, if metal clustering[7] dominates approaching the NM-M transition, the observed rise of $\overline{V}_{\rm K}(x)$, in the range $0.1\leqslant x\leqslant0.2$, implies an increase of the mean interatomic distance with the cluster size.

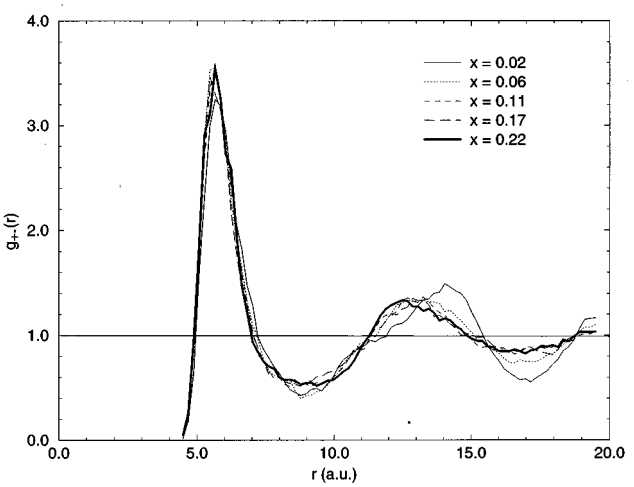

FIG. 1. Radial cation-anion pair correlation function of $K_x(KCl)_{1-x}$, at different excess metal concentrations.

The static structure of the electronic configurations can be characterized in terms of the radial pair correlation function between the electrons and the surrounding ions. This function is defined as

$$g_{e\pm}(r)=\frac{V_b}{4\pi r^2 N_e N_\pm}\left\langle\sum_{I_\pm}\int d\mathbf{r}'n(\mathbf{r}')\delta(|\mathbf{r}'-\mathbf{R}_{I_\pm}|-r)\right\rangle, \tag{5}$$

TABLE I. Averaged cation–closest-cation distance, R_{++}, as a function of x, for $K_x(KCl)_{1-x}$.

x	R_{++} (a.u.)
0.02	7.55
0.06	7.35
0.11	7.29
0.15	7.14
0.17	7.21
0.22	7.27

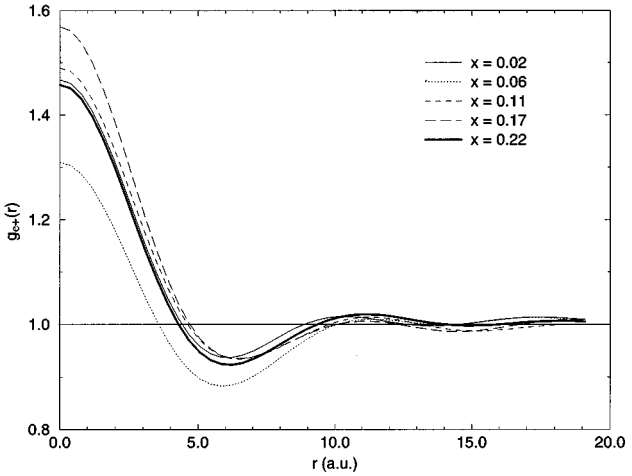

FIG. 2. Radial electron-cation pair correlation function of $K_x(KCl)_{1-x}$, at different excess metal concentrations.

where V_b is the volume of the simulation box, N_+ (N_-) the total number of cations (anions) to which the sum over I_+ (I_-) is extended, $\mathbf{R}_{I_+}$ ($\mathbf{R}_{I_-}$) are the cation (anion) coordinates, and the bracket indicates temporal average. The function $g_{e+}(r)$, for K-KCl, is shown in Fig. 2. As can be expected the probability of finding a cation close to a given electron is high. Furthermore, the behavior of this function does not change very much on increasing the excess metal concentration, with the exception of the case $x=0.06$. At this value of x the probability of finding a cation close to a given electron seems to be definitely lower than at the other metal concentrations.

In Fig. 3 we compare the radial electron-cation pair correlation functions of K-KCl and Na-NaBr, at two different metal concentrations, that is, $x=0.02$ and $x=0.17$. In both cases, there is a substantial difference between the two systems, related to the fact that the electron states are much more localized in Na-NaBr than in K-KCl. This is in agreement with the results of previous simulations.[22] We can introduce the mean coordination number Z_{e+}, defined as the value of the coordination function

$$Z_+(r)=\frac{4\pi N_+}{V_b}\int_0^r ds s^2 g_{e+}(s) \tag{6}$$

at the position of the first minimum of $g_{e+}(r)$. Z_{e+}, as a function of the metal concentration x, is reported in Table II. Both in K-KCl and in Na-NaBr, for most of the values of x, Z_{e+} is between 2 and 3, thus suggesting the formation of aggregates intermediate between M_2 and the real bipolaron, which should be characterized by a mean coordination number close to 4.[12–15] However, there are two remarkable exceptions. In K-KCl, for $x=0.06$, the value of Z_{e+} is only $\simeq 1.7$, indicating that also the K^- species has a significant probability to be formed. The peculiar behavior of the case $x=0.06$ has already been observed by considering the $g_{e+}(r)$ curves (see Fig. 2). In Na-NaBr, for $x=0.02$, $Z_{e+}\simeq 3.8$, so that, in this case, the bipolaron is definitely the most favored aggregate.

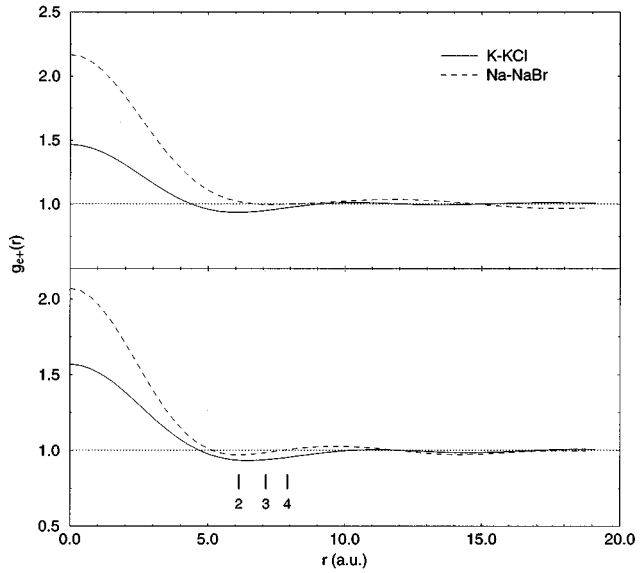

FIG. 3. Radial electron-cation pair correlation function of $K_x(KCl)_{1-x}$ and $Na_x(NaBr)_{1-x}$, at $x=0.02$ (upper panel) and $x=0.17$ (lower panel). A few values of the coordination function $Z_+(r)$ are indicated by vertical bars.

TABLE II. Mean coordination number Z_{e+} of $K_x(KCl)_{1-x}$ and $Na_x(NaBr)_{1-x}$, at different excess metal concentrations.

x	Z_{e+} (K-KCl)	Z_{e+} (Na-NaBr)
0.02	2.04	3.75
0.06	1.72	
0.09		2.60
0.11	2.03	
0.15	2.28	
0.17	2.28	2.38
0.22	2.06	

As far as Na-NaBr is concerned, our computed mean coordination numbers are in good agreement with the results reported in Ref. 22, while for K-KCl, Fois and co-workers[14,15] found slightly larger values, between 3 and 4, indicating a higher probability of bipolaronic complexes. This discrepancy could be related to some basic differences in the computational schemes. In particular we have taken into account the finite electronic temperature and, compared to the calculation of Ref. 14, our simulation box was significantly larger. However, as can be seen in Fig. 3 and in figures reported elsewhere,[14,15,22] the first minimum of the function $g_{e+}(r)$ is quite flat in the region where the coordination function goes from 2 to 4. Furthermore, we have used a sparse mesh, with a low spatial resolution. From these considerations it is evident that a very accurate estimate of Z_{e+} is impossible. Therefore the mentioned disagreement should not be overemphasized. Basically, our results, together with those obtained by others,[12,14,15,22] seem to suggest that, in metal–molten-salt solutions, the formation of different aggregates, that is, M^-, M_2, and bipolarons, is possible. By means of computer simulations, which use simple model systems, it is difficult to predict the relative frequency of these species with high accuracy. In spite of these limitations, we can conclude, in agreement with Ref. 22, that in Na-NaBr the electron charge is much more local-

TABLE III. HOMO-LUMO energy gap E_g (for comparison $k_BT=0.11$ eV), HOMO participation ratio p_H, electron density participation ratio p_n, and $R_p=p_{\max}/p_H$, of $K_x(KCl)_{1-x}$, at different excess metal concentrations. Statistical errors, in the last digit, are shown in brackets.

x	E_g (eV)	p_H	p_n	R_p
0.02	0.64(9)	0.025(1)	0.028(1)	3.68
0.06	0.14(3)	0.044(2)	0.088(2)	1.91
0.11	0.13(3)	0.060(2)	0.156(2)	1.87
0.15	0.08(1)	0.075(4)	0.206(2)	1.47
0.17	0.06(1)	0.086(2)	0.221(3)	1.51
0.22	0.07(1)	0.120(3)	0.300(2)	1.30

ized than in K-KCl. Of course this behavior is due to the different strength of the cation-electron pseudopotentials. The Na^+ electron pseudopotential is significantly more attractive than the K^+ electron one, in line with the related values of the first ionization energies of Na and K. Hence, in Na-NaBr and K-KCl, the observed different localization of the electronic charge is clearly to be expected.

B. Electronic state properties

On approaching the NM-M transition, the delocalization of the electron density occurs concomitantly with a decrease of the energy gap and an increase of the density of states at the Fermi level. This can be clearly seen in Tables III and IV, where the configurational averages of some electronic state properties are given, and in Fig. 4, which shows the single-particle density of states $N(E)$ in K-KCl. The energy gap is defined as what would, in a BO simulation, be called the HOMO-LUMO gap, that is, $E_g=E_{(N_e/2+1)}-E_{(N_e/2)}$, where E_i denotes the single-particle energy of the ith state. At the temperature we have considered, namely, 1300 K, $k_BT=0.11$ eV, so that for $x=0.02$ on average E_g is much larger than k_BT and a nonmetallic behavior is to be expected. However, in agreement with Ref. 14, we have found that, for some ionic configurations, the energy gap decreases to values not much higher than k_BT, thus making a low electronic conductivity possible by means of electron jumping.[14] In Na-NaBr, at $x=0.02$, E_g is much higher than in K-KCl and this clearly suggests that Na-NaBr has a stronger electronic state localization than K-KCl. By increasing the excess metal concentration E_g becomes smaller and, for $x>0.1$, both in K-KCl and Na-NaBr, its value decreases below k_BT. Then the system starts showing a metallic behavior.

TABLE IV. HOMO-LUMO energy gap E_g (for comparison $k_BT=0.11$ eV), HOMO participation ratio p_H, electron density participation ratio p_n, and $R_p=p_{\max}/p_H$, of $Na_x(NaBr)_{1-x}$, at different excess metal concentrations. Statistical errors, in the last digit, are shown in brackets.

x	E_g (eV)	p_H	p_n	R_p
0.02	1.07(9)	0.018(1)	0.018(1)	6.44
0.09	0.12(1)	0.039(2)	0.108(1)	2.10
0.17	0.09(1)	0.071(4)	0.189(2)	1.66

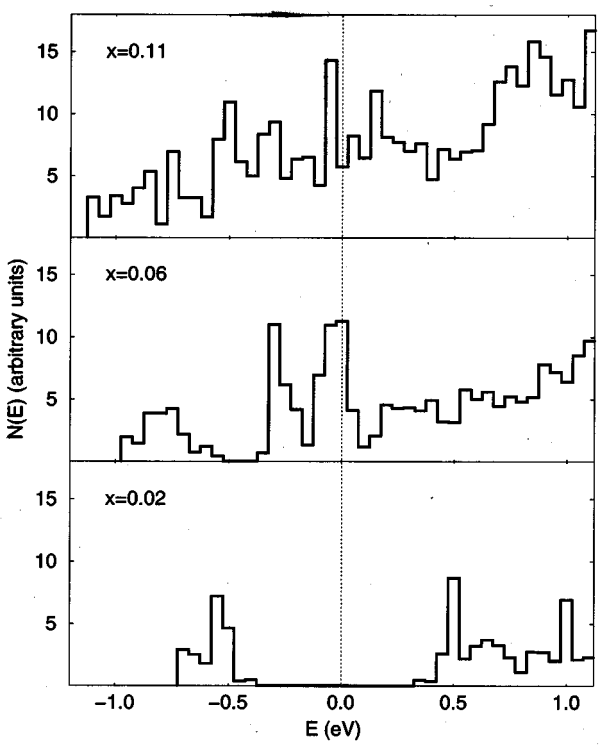

FIG. 4. Single-particle density of states $N(E)$ in $K_x(KCl)_{1-x}$, at different excess metal concentrations, calculated by averaging over 1000 configurations. The chemical potential μ has been set to zero for each configuration.

A similar trend can be observed in the single-particle electronic density of states $N(E)$ (Fig. 4). This quantity has been calculated by averaging over the eigenvalues of 1000 ionic configurations (the chemical potential μ has been set to zero for each configuration). Since in our simulations, only a few states are computed, there is likely a large error in the detailed shape of $N(E)$. Moreover, our limited energy resolution prevents us from getting an accurate estimate of the NM-M transition point. However, at least qualitatively, the different behavior of the density of states around μ is evident. In this region, for $x=0.02$, $N(E)$ is equal to zero indicating that the system is not metallic at this low concentration. For $x=0.06$ the density of states becomes nonzero at μ; however, it has deep minima just below and above μ, thus suggesting that the system is not a true metal. In contrast, for $x=0.11$ (and higher values, of course), the density of states clearly exhibits a metallic behavior.

In order to get more information about the localization of the electronic states we have also computed the HOMO participation ratio,

$$p_H=\left[V_b\int_{V_b}d\mathbf{r}|\psi_{Ne/2}(\mathbf{r})|^4\right]^{-1}, \tag{7}$$

and the electron density participation ratio

$$p_n=N_e^2/V_b\left[\int_{V_b}d\mathbf{r}n(\mathbf{r})^2\right]^{-1}. \tag{8}$$

The electron density can be expressed in terms of the single-particle orbitals,

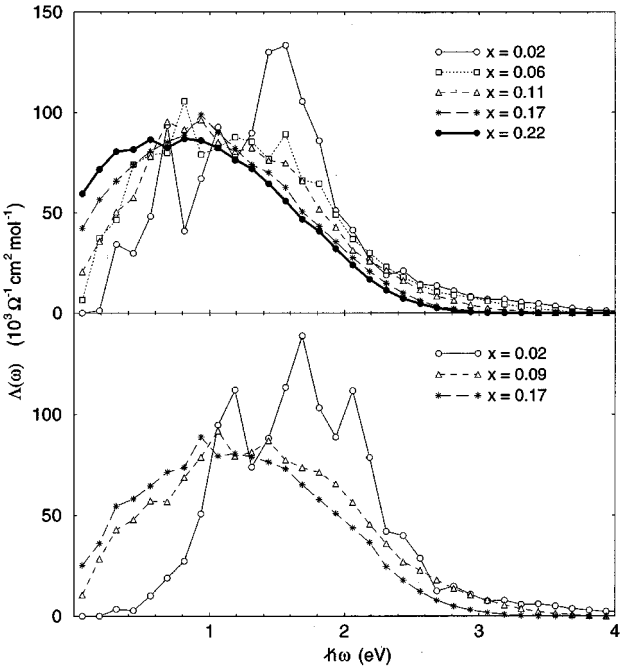

FIG. 5. Equivalent optical conductivity, for $K_x(KCl)_{1-x}$ (upper panel) and $Na_x(NaBr)_{1-x}$ (lower panel), at different excess metal concentrations. Symbols represent calculated values (averaging over 80 uncorrelated ionic configurations), while the lines are just a guide for the eye.

$$n(\mathbf{r}) = \sum_i f_i |\psi_i(\mathbf{r})|^2, \tag{9}$$

where f_i are the Fermi-Dirac occupation numbers. The configurational averages of these participation ratios are reported in Tables III and IV. p_H and p_n are defined in such a way that their values are always smaller than 1, being equal to 1 for a perfectly delocalized HOMO or electronic density. By considering the participation ratios of all the computed states, the presence of a mobility edge can be revealed. In fact, if the participation ratio values are quite different (indicating that some states are localized while the others are delocalized) a mobility edge is present, and the system is metallic if the mobility edge is located below the Fermi level. Therefore, in Tables III and IV we have reported the quantity $R_p = p_{\max}/p_H$, where $p_{\max}$ is the participation ratio of the highest excited state computed in the simulation (if the number of computed excited states is large enough one can assume that the highest state is always delocalized for all the metal concentrations we have considered). As can be seen, R_p decreases by increasing x in such a way that, for $x > 0.11$, the electronic states at the Fermi level are not much more localized than the highest one. As expected from previous considerations, in Na-NaBr, both the HOMO and the density participation ratios have smaller values than in K-KCl, thus denoting again a stronger electron state localization.

The structure of the electronic states is reflected in the optical absorption spectra which can be obtained by computing the frequency-dependent electrical conductivity $\sigma(\omega)$. As in Refs. 14,15,22, we use the Kubo-Greenwood relation to evaluate the spectrum for a fixed ionic configuration,

TABLE V. dc electrical conductivity of $K_x(KCl)_{1-x}$ and $Na_x(NaBr)_{1-x}$, at different excess metal concentrations. Statistical errors, in the last digits, are shown in brackets.

x	σ (K-KCl)	σ (Na-NaBr)
0.02	0	0
0.06	1(1)	
0.09		6(3)
0.11	30(8)	
0.15	56(15)	
0.17	120(16)	68(16)
0.22	242(10)	

$$\sigma(\omega, R_I) = \frac{2\pi e^2}{3m^2\omega} \frac{1}{V_b} \sum_{i,j} (f_i - f_j) |\langle \psi_i | \hat{p} | \psi_j \rangle|^2 \times \delta(E_j - E_i - \hbar\omega), \tag{10}$$

where e and m are the electronic charge and mass, $\hat{p}$ is the momentum operator, and ψ_i, E_i, are the electronic DFT eigenstates and eigenvalues, calculated for the ionic configuration $\{R_I\}$. Of course, the use of the single-particle DFT states and eigenvalues, instead of the true many-body eigenfunctions and eigenvalues, introduces an approximation. Then $\sigma(\omega)$ can be computed averaging over several ($\simeq 80$) uncorrelated configurations. In Fig. 5 we plot the equivalent optical conductivity,

$$\Lambda(\omega) = \sigma(\omega)/n_e, \tag{11}$$

where n_e is the average excess electron density. The behavior of $\Lambda(\omega)$ at different excess metal concentrations is in good agreement with the optical spectra obtained by experiments[6,11,23] and previous computer simulations,[14,15,22] although our $\Lambda(\omega)$ functions exhibit sharp features (particularly at $x = 0.02$) that can be attributed to our limited sampling. For instance, in Na-NaBr, at $x = 0.02$, the energy of the absorption maximum [the highest peak of $\Lambda(\omega)$] is found at 1.69 eV to be compared with the experimental value[11] of 1.65 eV. Furthermore, the $\Lambda(\omega)$ curves are slightly more symmetric in Na-NaBr than in K-KCl, in qualitative agreement with the experimental findings[11] which suggest that, at low excess metal concentration, only one Gaussian is necessary to fit the optical spectra of Na-NaBr, in contrast to the K-KCl spectra which can be reproduced by two Gaussians of comparable magnitude. As can be seen from Fig. 5, the equivalent conductivity curves differ mostly in the low-frequency region where the enhancement of $\Lambda(\omega)$ with x reflects a related increase of the dc electrical conductivity σ. This quantity can be computed by extrapolating $\sigma(\omega)$ to zero frequency,

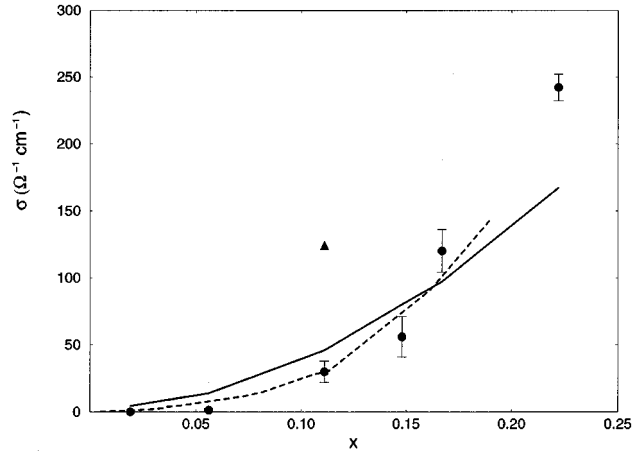

FIG. 6. dc electrical conductivity σ of $K_x(KCl)_{1-x}$, at different excess metal concentrations. The solid and dashed lines connect points taken from two sets of experimental data (Refs. 8 and 21) obtained at slightly different experimental conditions. The full circles (with their error bars) are our simulation results, while the triangle represents the estimate obtained by Fois, Selloni, and Parrinello (Ref. 15) for $x=0.11$ by making use of the BO approximation.

$$\sigma=\sigma(0)=\lim_{\omega\to 0}\sigma(\omega). \tag{12}$$

The behavior of σ, as a function of x, is illustrated in Table V and in Fig. 6. As far as K-KCl is concerned, in spite of the crudeness of our model and of the approximations involved in the calculation of σ, the agreement between the results of our simulations and the experimental data[8,21] is satisfactory. Notice that at $x=0.11$, our computed dc conductivity is much closer to the corresponding experimental data than the estimate obtained by the simulation of Fois, Selloni, and Parrinello,[15] who used the BO approximation.

For Na-NaBr, to our knowledge, only experimental measurements[21] of σ, performed at low excess metal concentrations ($x<0.1$), are available. The reported[21] dc electrical conductivities[36] are 0.5 and 15 Ω^{-1} cm^{-1} for $x=0.02$ and $x=0.09$, respectively. These values are close enough to our simulation results given in Table V. As expected, the dc electrical conductivity strongly depends on the delocalization of the electronic states around the Fermi level and on the size of the energy gap. By increasing x, the energy gap is reduced and the density of states at the Fermi level becomes nonzero, the relevant electronic states being delocalized. As a consequence, σ increases very rapidly and the NM-M transition can take place. We notice that, according to the Mott minimum metallic conductivity criterion,[16] the NM-M transition should occur[8] when $\sigma\simeq 150\,\Omega^{-1}$ cm^{-1}. Therefore, considering our data, we could locate the NM-M transition of K-KCl within a range of metal concentrations going from 0.17 to 0.22. By comparing the σ values of K-KCl and Na-NaBr, at similar excess metal concentrations, it is evident that the dc electrical conductivity is significantly lower in Na-NaBr. This behavior, which is in agreement with the experimental findings,[2,5,11,21–23] is related to the different degree of delocalization of the electronic states, a feature we have already discussed by means of the participation ratios.

TABLE VI. Average occupation numbers, for the HOMO and LUMO of $K_x(KCl)_{1-x}$, at different excess metal concentrations.

x	f_{HOMO}	f_{LUMO}
0.02	0.91	0.09
0.06	0.64	0.36
0.11	0.61	0.34
0.15	0.58	0.40
0.17	0.56	0.42
0.22	0.57	0.42

We conclude this section by reporting, in Table VI, the average occupation numbers of the HOMO and LUMO of K-KCl. The effect of the finite electronic temperature, which makes the Fermi-Dirac distribution function smooth, is evident. Notice that, in a BO simulation, one would assume that $f_{\mathrm{HOMO}}=1$ and $f_{\mathrm{LUMO}}=0$.

C. Percolating structures and the NM-M transition

The NM-M transition should be characterized by the formation of conducting percolating paths. This process can be easily recognized by looking at the electronic density distributions drawn in Fig. 7, which shows snapshots of our simulation system, with representative configurations which have been selected for some excess metal concentrations in K-KCl. It is evident that, for $x=0.02$, the electronic density is localized in a bipolaronic structure. For $x=0.11$ the bipolarons begin to associate and form clusters. For $x=0.17$ a percolating cluster, extending throughout the entire simulation cell, is formed. Finally, for $x=0.22$, the electrons are delocalized in a multitunnel-like structure, indicating that the system is becoming a real liquid metal.

We notice that an analogous behavior has been observed by Deng, Martyna, and Klein,[37] who performed computer simulations to study the NM-M transition of solutions of metals in liquid ammonia. This suggests a strong similarity between metal–molten-salt solutions and metal-ammonia solutions, in agreement with the experimental evidence.[3]

As in Ref. 15 we quantitatively distinguish between percolating and nonpercolating structures using the following algorithm. We consider a particular ionic configuration and we place a set of random walkers on the points of our real-space mesh. These random walkers are allowed to move on the subset of the points of the real-space mesh where the electronic charge density $n(\mathbf{r})$ is greater than some threshold value n_t. If they arrive at a site where $n(\mathbf{r})<n_t$ they are reflected. One can evaluate the mean-square displacement, $\langle d^2\rangle$, of such walkers. Percolating structures, in which there is a connected path between one side and the other of the cell, will display a diffusive behavior of $\langle d^2\rangle$ (that is $\langle d^2\rangle$ will always increase), while in nonpercolating structures $\langle d^2\rangle$ will eventually saturate to a constant value. Then the whole procedure can be repeated by considering many uncorrelated ionic configurations. n_t was taken to be 1/10 of the maximum value of $n(\mathbf{r})$ on the grid. Reasonable variations of n_t gave qualitatively similar results. In Table VII we report the fraction of percolating configurations found in K-KCl and Na-NaBr, at different excess metal concentrations. In K-KCl, at $x=0.02$, no percolating structures are

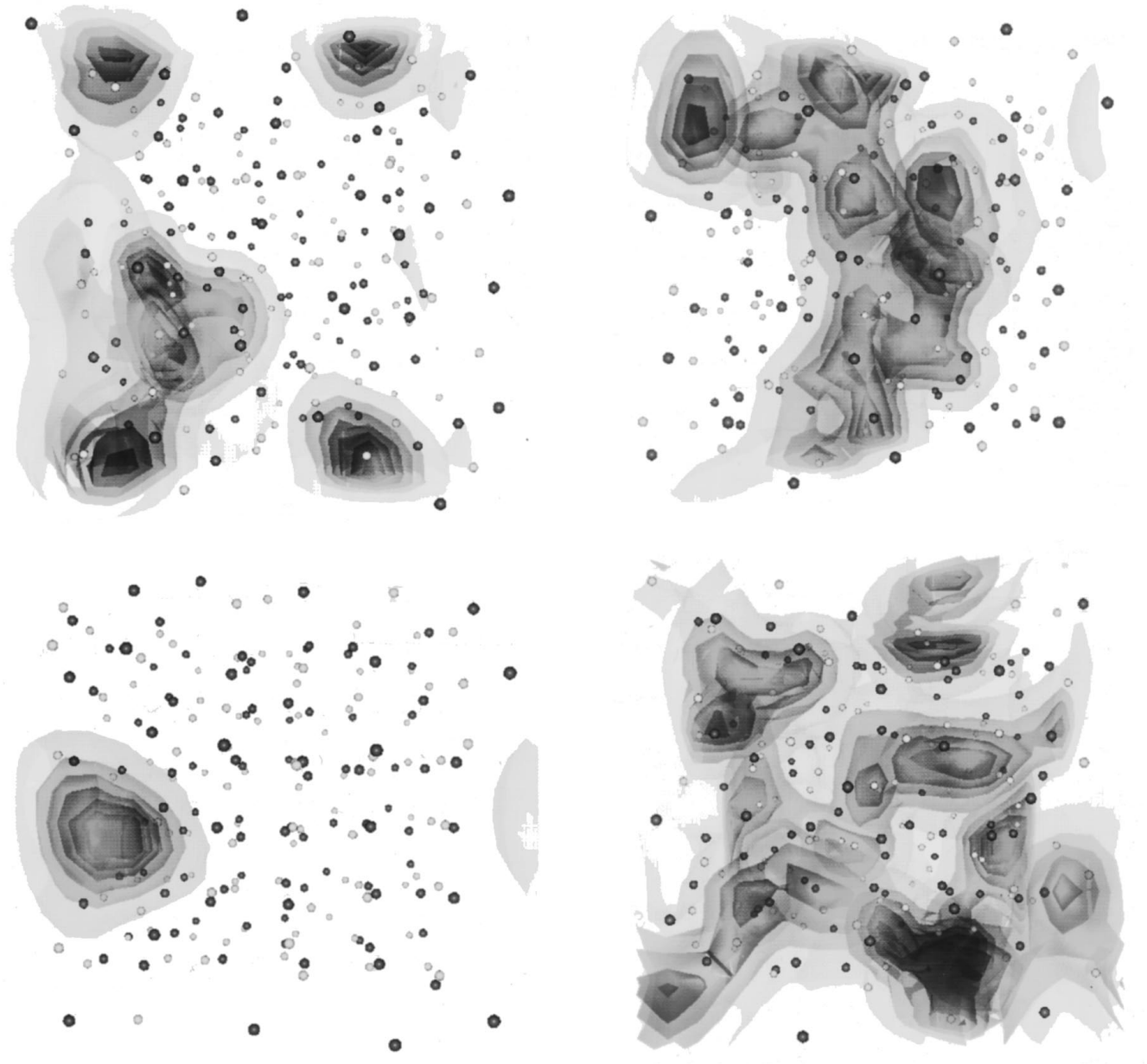

FIG. 7. Electron density distributions of representative configurations of $K_x(KCl)_{1-x}$, at $x=0.02$ (bottom left), $x=0.11$ (top left), $x=0.17$ (top right), and $x=0.22$ (bottom right).

observed. At $x=0.06$ the probability of finding a percolating configuration is quite low, while it becomes high for $x \geqslant 0.11$. For $x \geqslant 0.17$ essentially all the configurations exhibit a percolating behavior and the system is expected to be in the metallic regime. Therefore $x=0.17$ could be considered as an upper limit for the concentration at which the NM-M transition occurs. In Na-NaBr, as a consequence of the higher electronic charge localization, the fraction of percolating configurations is smaller than in K-KCl, at similar values of x. This also suggests that the NM-M transition takes place in Na-NaBr at higher excess metal concentration than in K-KCl.

A similar analysis can be carried out by looking at the fluctuations of the electronic charge density. To this aim we have divided our simulation box into N_c smaller cubic cells and we have computed the average electron density, n_l, within each cell, that is,

$$n_l = \frac{1}{M} \sum_i n(\mathbf{r}_i), \tag{13}$$

where the sum is extended to all the M mesh points contained in the lth cell, and l goes from 1 to N_c. Then the electron density fluctuations can be estimated by evaluating the standard deviation,

$$s = \left(\frac{\langle n^2 \rangle - \langle n \rangle^2}{N_c} \right)^{1/2}, \tag{14}$$

where $\langle n^p \rangle$ is given by

$$\langle n^p \rangle = \frac{1}{N_c} \sum_l n_l^p . \tag{15}$$

TABLE VII. Fraction of percolating configurations in $K_x(KCl)_{1-x}$ and $Na_x(NaBr)_{1-x}$, at different excess metal concentrations.

x	K-KCl	Na-NaBr
0.02	0.00	0.00
0.06	0.10	
0.09		0.17
0.11	0.85	
0.15	0.95	
0.17	1.00	0.70
0.22	1.00	

In Fig. 8 the behavior of s as a function of x is plotted in the case of K-KCl, using $N_c=64$. s is averaged over 80 uncorrelated ionic configurations. As expected, the electron density fluctuations decrease by increasing the excess metal concentration, since the electron states become more delocalized and the electronic charge more uniformly distributed within the simulation box. Of course the reduction of the density fluctuations is closely related to the formation of extended, percolating paths.

The three-dimensional character of the percolating structures can be investigated by considering the matrix $J_{\alpha\beta}$, similar to the moment of inertia tensor, defined as

$$J_{\alpha\beta}=\langle d^2\rangle\delta_{\alpha\beta}-\langle d_\alpha d_\beta\rangle \quad \alpha,\beta=x,y,z, \tag{16}$$

where d_α is the αth component of the displacement of a single random walker and brackets indicate averages performed over all the random walkers. One can define the quantity

$$W=\frac{(w_2+w_3)/2-w_1}{w_1}, \tag{17}$$

where $w_1\leqslant w_2\leqslant w_3$ are the eigenvalues of $J_{\alpha\beta}$, averaged over the random walker propagation steps and over many uncorrelated configurations. Obviously $W\simeq 0$ for a true three-dimensional electronic distribution. In Table VIII we

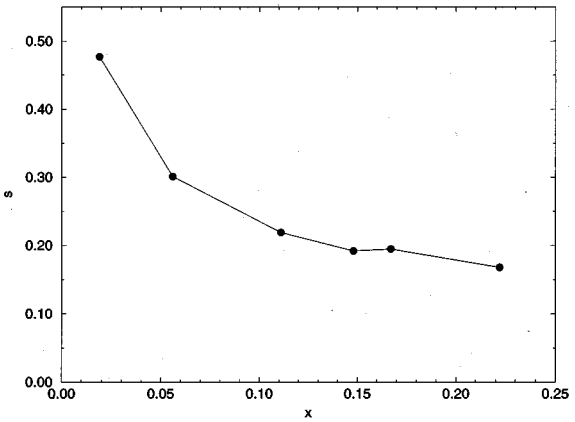

FIG. 8. Standard deviation (see text for the definition) of the electronic charge density, in $K_x(KCl)_{1-x}$, at different excess metal concentrations. Symbols represent calculated values (averaging over 80 uncorrelated ionic configurations), while the line is just a guide for the eye.

TABLE VIII. W (see text for the definition) indicating the three-dimensional character of the percolating configurations in $K_x(KCl)_{1-x}$ and $Na_x(NaBr)_{1-x}$, at different excess metal concentrations.

x	W (K-KCl)	W (Na-NaBr)
0.06	9.44	
0.09		7.66
0.11	3.43	
0.15	1.92	
0.17	1.37	2.14
0.22	0.51	

report the values of W, computed by taking into account the percolating configurations only. As can be seen W decreases rapidly by increasing the excess metal concentration and this shows that the percolating structures become more and more three dimensional. In particular, at $x=0.22$ in $K_x(KCl)_{1-x}$, the three-dimensional character is very pronounced.

VI. CONCLUSIONS

In summary, we have used the method of *ab initio* MD, based on finite-temperature DFT, to study electronic and structural properties of two metal–molten-salt solutions, K-KCl and Na-NaBr. Our technique allowed us to perform MD simulations at excess metal concentrations much higher than in the previous studies and to reproduce the basic features of the NM-M transition observed in the experiments.

As the electron concentration increases, the character of the electron density changes from localized to extended. At low metal concentrations, the excess electrons localize, and the formation of small aggregates like M_2, M^-, and bipolarons is possible. At higher concentrations the electrons start to cluster and form elongated structures. Next, the electron density becomes completely delocalized. This process is accompanied by a decrease in the energy gap and an increase of the density of states at the Fermi level. As a consequence, the system exhibits a significant dc electrical conductivity, which indicates the onset of the metallic regime. Since the delocalization of the electronic states gives rise to percolating conducting paths, the basic features of the NM-M transition can be described in terms of a volume-percolation process.

As far as the identification of the NM-M transition region is concerned, our estimates, based on the study of different physical properties, locate the critical excess metal concentration within the range $0.11<x<0.20$, for K-KCl. This result is in reasonable agreement with the experiments and the calculations performed using the percolation theory approach, even though our predicted critical concentration is slightly lower than most of the other estimated values. This could be due to our small simulation box. Experimental measurements[6] predict a dielectric catastrophe at $x\simeq 0.10$, but it is believed[7,18] that this effect simply indicates the presence of sizable metallic clusters, the system still being in the

nonmetallic phase. Our simulation box is possibly too small to distinguish between a solution characterized by large metallic clusters and a real liquid metal.

Finally, by comparing the results obtained for K-KCl and Na-NaBr, we have found remarkable differences between the two systems. In particular, the electronic states are much more localized in Na-NaBr. Therefore, for a given value of x, the computed dc electrical conductivity is lower in Na-NaBr than in K-KCl, in agreement with the experimental data. Furthermore we predict that, in Na-NaBr, the NM-M transition occurs at higher metal concentration than in K-KCl. Basically, this anomalous behavior of the Na-NaX systems is caused by the strong attractive interaction between the Na^+ ions and the excess electrons.

ACKNOWLEDGMENTS

The work of the FOM Institute is part of the research program of FOM and is supported by the Netherlands Organization for Scientific Research (NWO). Supercomputer time was made available through a grant by the Dutch National Foundation for Computing Facilities (NCF). P.L.S. would like to thank the Max-Planck-Institut für Festkörperforschung, where part of this work was done, for their hospitality.

*Present address: Max-Planck-Institut für Festkörperforschung, Heisenbergstr. 1, 70569 Stuttgart, Germany.

[1] For a general review see, for instance, P. P. Edwards, T. V. Ramakrishnan, and C. N. R. Rao, J. Phys. Chem. **99**, 5228 (1995), and references quoted therein.

[2] M. A. Bredig, *Molten Salt Chemistry*, edited by M. Blander (Interscience, New York, 1964).

[3] P. Chieux, P. Damay, J. Dupuy, and J. F. Jal, J. Phys. Chem. **84**, 1211 (1980).

[4] N. Nicoloso and W. Freyland, Z. Phys. Chem. Neue Folge **135**, 39 (1983).

[5] W. W. Warren, Jr., S. Sotier, and G. F. Brennert, Phys. Rev. Lett. **50**, 1505 (1983).

[6] W. Freyland, K. Garbade, and E. Pfeiffer, Phys. Rev. Lett. **51**, 1304 (1983).

[7] N. Nicoloso and W. Freyland, J. Phys. Chem. **87**, 1997 (1983).

[8] D. Nattland, H. Heyer, and W. Freyland, Z. Phys. Chem. **149**, 1 (1986).

[9] W. W. Warren, Jr., B. F. Campbell, and G. F. Brennert, Phys. Rev. Lett. **58**, 941 (1987).

[10] K. Garbade and W. Freyland, Z. Phys. Chem. **156**, 169 (1988).

[11] D. Nattland, Th. Rauch, and W. Freyland, J. Chem. Phys. **98**, 4429 (1993).

[12] M. Parrinello and A. Rahman, J. Chem. Phys. **80**, 860 (1984).

[13] A. Selloni, P. Carnevali, R. Car, and M. Parrinello, Phys. Rev. Lett. **59**, 823 (1987).

[14] E. S. Fois, A. Selloni, M. Parrinello, and R. Car, J. Phys. Chem. **92**, 3268 (1988).

[15] E. Fois, A. Selloni, and M. Parrinello, Phys. Rev. B **39**, 4812 (1989).

[16] N. F. Mott, *Metal-Insulator Transitions* (Taylor & Francis, London, 1974).

[17] W. W. Warren, Jr., in *The Metallic and Non-Metallic States of Matter: An Important Facet of the Chemistry and Physics of The Condensed State*, edited by P. P. Edwards and C. N. R. Rao (Taylor & Francis, London, 1985).

[18] G. Senatore and M. P. Tosi, Philos. Mag. B **51**, 267 (1985), and references quoted therein.

[19] A. Alavi, J. Kohanoff, M. Parrinello, and D. Frenkel, Phys. Rev. Lett. **73**, 2599 (1994).

[20] N. D. Mermin, Phys. Rev. **137**, A1441 (1965).

[21] H. R. Bronstein and M. A. Bredig, J. Am. Chem. Soc. **80**, 2077 (1958).

[22] L. F. Xu, A. Selloni, and M. Parrinello, Chem. Phys. Lett. **162**, 27 (1989).

[23] W. Freyland, K. Garbade, H. Heyer, and E. Pfeiffer, J. Phys. Chem. **88**, 3745 (1984).

[24] N. Yu, P. Xia, L. A. Bloomfield, and M. Fowler, J. Chem. Phys. **102**, 4965 (1995).

[25] W. W. Warren, Jr., S. Sotier, and G. F. Brennert, Phys. Rev. B **30**, 65 (1984).

[26] J. Jal, Doctoral thesis, Université Claude Bernard-Lyon I, 1981.

[27] G. J. Morgan, R. Gilbert, and B. J. Hickey, J. Phys. F **15**, 2171 (1985).

[28] See, for instance, A. L. Efros and B. I. Shklovskii, Phys. Status Solidi B **76**, 475 (1976).

[29] W. Hefner and F. Hensel, Phys. Rev. Lett. **48**, 1026 (1982).

[30] D. J. Bergman, Phys. Rev. Lett. **44**, 1285 (1980).

[31] T. E. Faber and J. M. Ziman, Philos. Mag. **11**, 153 (1965), and references quoted therein.

[32] D. E. Logan, Phys. Rev. Lett. **57**, 782 (1986).

[33] F. G. Fumi and M. P. Tosi, J. Phys. Chem. Solids **25**, 31 (1964); **25**, 45 (1964).

[34] R. W. Shaw, Phys. Rev. **174**, B760 (1968).

[35] D. M. Ceperley and B. J. Alder, Phys. Rev. Lett. **45**, 566 (1980).

[36] In order to get the dc electronic conductivity from the total dc conductivity measured experimentally, we subtract the ionic contribution which is assumed to be the same as for the pure molten salt, that is, $\sigma = \sigma_{\mathrm{tot}} - \sigma_{\mathrm{ion}}$.

[37] Z. Deng, G. J. Martyna, and M. L. Klein, Phys. Rev. Lett. **71**, 267 (1993).